Origin of the Opalescence at the $\alpha - \beta$ Transition of Quartz: Role of the Incommensurate Phase Studied by Synchrotron Radiation

G. Dolino,[1,*] P. Bastie,[1] B. Capelle,[2] V. Chamard,[3] J. Härtwig,[4] and P. L. Guzzo[5]

[1]*Laboratoire de Spectrométrie Physique (UMR 5588), Université Joseph Fourier, BP 87, 38402 Saint-Martin d'Hères Cedex, France*
[2]*Laboratoire de Minéralogie et Cristallographie (UMR 7590), Université Pierre et Marie Curie, 75320 Paris Cedex 05, France*
[3]*Laboratoire de Thermodynamique et Physico-Chimie Métallurgiques (UMR 5614), 38402 Saint-Martin d'Hères, France*
[4]*European Synchrotron Radiation Facility, BP 220, 38043 Grenoble Cedex, France*
[5]*Departamento de Engenharia de Minas, Universidade Federal de Pernambuco Cidade Universitária, 50740-530 Recife, PE, Brazil*
(Received 16 December 2004; published 18 April 2005)

The origin of the light scattering observed at the $\alpha - \beta$ transition of quartz is still a subject of controversy. We present structural studies performed during the coexistence of the α and the intermediate incommensurate (inc) phases using simultaneously synchrotron x-ray diffraction and optical techniques. The small and large angle light scatterings are due, respectively, to the orientation domains of the $3q$ inc phase and to the α phase twins revealed by diffuse x-ray scattering. In the vicinity of the interphase boundary, the two light scattering regions, both with perturbed properties, form a complex multiscale structure.

PACS numbers: 64.70.Rh, 61.10.Nz, 78.35.+c

At the end of the last century, the field of structural phase transitions was marked by great progress in the theory of critical behaviors of continuous transitions [1]. However, most crystal transitions are first order and are driven by the nucleation and motion of a phase interface. Metastable structures are often produced, particularly in metallic alloys, either with composition variations or without as in diffusionless martensitic materials [2]. Because of their small size, the initial metastable structures are generally observed by transmission electron microscopy (TEM) or diffuse x-ray scattering. In transparent crystals with weak first order transition, larger interfacial structures may be observed by optical measurements [3]. The $\alpha - \beta$ transition of quartz deserves special attention due to many important results obtained during a century of research [4]. However, the observation in 1956 of an intense transition opalescence by Yakolev *et al.* [5] remains an unresolved question which is still a subject of controversy, recently reviewed by two of us [6]. The aim of the present work is to determine the microscopic structures at the origin of this light scattering (LS).

The quartz opalescence was first attributed to the effect of dynamical fluctuations [5], but this hypothesis was discarded after the observation of static speckles by Shapiro and Cummins [7]. In addition to this large angle scattering (LAS), a small angle scattering (SAS) was observed in an adjacent region [8]. Both LSs are anisotropic, being produced by cylinders parallel to the trigonal Z axis, with sections in the 1 and the 20 μm range, respectively. The origin of these LSs remained unexplained until the discovery of the incommensurate (inc) phase of quartz [9], predicted by Aslanyan and Levanyuk [10]. This opened the way to the LS models developed recently by Saint-Grégoire *et al.* [11] and Aslanyan *et al.* [12], introducing the existence of different ferroelastic inc phases. A third model is based on the facts that the α-inc transition is first

order and that LS is observed only during the α-inc coexistence [6]. Inhomogeneous coexistence states with various triangular structures are indeed observed by TEM in thin samples, perpendicular to the Z axis [13–15]. A difference of 3 orders of magnitude in sample size prevents one to establish a direct link between these microscopic structures and the two LS regions; this becomes possible by using diffraction of high energy x rays in a macroscopic sample. A preliminary study with a laboratory hard x-ray source [16] showed the necessity to use high resolution synchrotron radiation.

Two quartz samples with polished faces perpendicular to the X, Y, and Z axes and similar transition properties are investigated: Sx is a synthetic crystal grown by SICN (France) and Ny is a natural crystal from Madagascar. Classical white beam x-ray topography is performed on the ID19 beam line of the European Synchrotron Radiation Facility (ESRF), in the transmission geometry using a high energy beam (about 50 keV). The diffraction patterns from an incident beam at a few degrees from the X (or Y) axis are recorded on photographic films or with a FRELON x-ray camera well suited for real time studies [17]. Continuous optical observations are performed along the Z axis with a white light beam and a CCD camera. In addition for Ny, we measure the LS from a HeNe laser beam, at an incidence of 3° with respect to the Z axis [8], focused in the middle of the sample at the same height as the x-ray beam. The quartz sample is placed in the furnace used for previous optical and x-ray measurements of the quartz inc phase with a temperature resolution of 1 mK [18]; however, there is a vertical temperature gradient of about 0.1 K/cm along the sample.

An overview of the α-inc phase transition in the sample Sx is presented in Fig. 1. The inc phase is characterized by the presence of 12 first order satellites exhibited in the inset of Fig. 1(a). Although only six satellites are expected in a
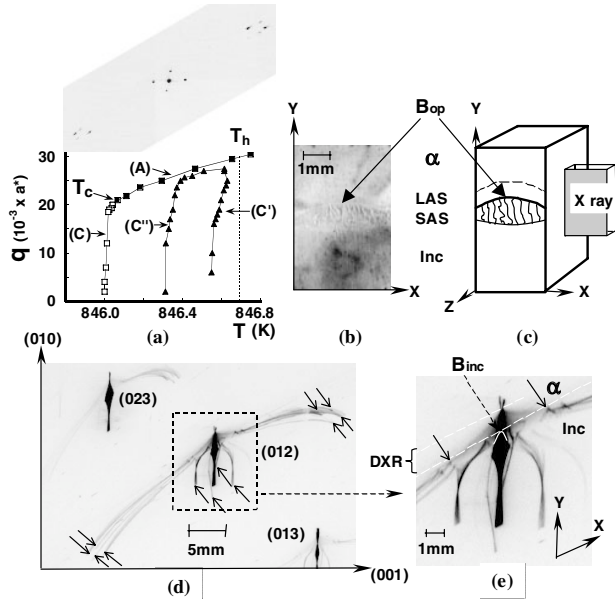
FIG. 1.   Overview of the α-inc transition of quartz in the sample Sx. (a) Temperature variations of the modulus of the inc wave vector q: curve (A), upon cooling from T_h to T_c in the inc phase; curve (C), in the transient coexistence state, obtained after nucleation of the α phase at T_c; curves (C') and (C''), in the stabilized coexistence state, on heating and cooling, respectively. Inset: x-ray diffraction pattern of the (012) lattice spot with its 12 satellites in the inc phase close to T_c. (b) Optical photography of the α-inc coexistence state (after heating), showing the SAS region and its upper boundary B_{op}. (c) A sketch of the sample Sx $(4.5 \times 14 \times 10 \text{ mm}^3$ along X, Y, and Z), showing the two regions (SAS and LAS) in the α-inc coexistence state (after heating), and the position of the incident x-ray beam. (d) Laue diagram of the coexistence state (after heating), exhibiting the spatial variation of the inc satellites, where the lower positions are indicated by 12 arrows. This picture is obtained on a photographic film at 67 cm from the sample, with an x-ray beam defined by a $0.2 \times 7 \text{ mm}^2$ ($H \times V$) slit. (e) Magnified central part of the (012) Laue diagram, showing the phase boundary B_{inc}, with the discontinuity of two symmetric satellites indicated by the arrows. There is a diffuse x-ray scattering region between the two oblique dashed lines.

hexagonal crystal, twice this number is observed due to the presence of rotation domains in the inc phase of quartz [6]. The inc wave vector (perpendicular to the Z axis) is defined by the modulus q and the angle ϕ relative to a^*, determined with a Laue simulation program [19] (a^* is a unit vector of the hexagonal reciprocal lattice, parallel to one of the Y axes). Upon heating, there is a first order transition at a temperature $T_h = 846.7$ K to the $3q$ inc phase which is present up to $T_i = 847.4$ K [6]. The transition to the β phase occurs with an intermediate $1q$ inc phase, usually present in a temperature range of 0.05 K around T_i [6,18].

Curve (A) of Fig. 1(a) shows the decrease of q in the inc phase, upon cooling from T_h to $T_c = 846$ K, the temperature of the first order lock-in transition to the α phase (where $q = 0.020a^*$ and $\phi = 7°$), with a thermal hysteresis $T_h - T_c = 0.7$ K, a little lower than the usual hysteresis

range of 1 K [6,7]. The lock-in transition at T_c starts with a single nucleation of the α phase at the colder top surface of the sample. A continuous motion of a single α-inc interface then follows. The corresponding decrease of q is plotted on curve (C), exhibiting a final discontinuity of $q = 0.002a^*$ while reaching the α phase. The α-inc coexistence state is easily stabilized with a quick increase of the furnace temperature by 0.5 K, just after the α phase nucleation at T_c [6]. A typical optical picture of the static coexistence state, obtained after heating, is presented in Fig. 1(b), exhibiting the vermicular texture of the SAS region, limited by a well defined upper boundary B_{op}. Figure 1(c) is a sketch of this coexistence state, showing also the position of the LAS region and the shape of the white x-ray beam covering the whole region from the α phase to the unperturbed inc phase. The corresponding Laue diagram is plotted in Figs. 1(d) and 1(e). One can note the deformation of the lattice spots showing the strain distribution resulting from the difference in lattice parameters between the α and the inc phases. The most spectacular feature is the observation of 12 convergent lines resulting from the spatial variation of the inc satellites: on the upper side, there is a discontinuity of $q = 0.006a^*$, defining unambiguously the boundary B_{inc} of the inc phase. Finally, a region of diffuse x-ray scattering at small q is observed above B_{inc}.

A spatially resolved investigation of the perturbed regions coexisting on the two sides of B_{inc} is now presented. It is performed around the (012) Laue spot with a fine x-ray beam during the α-inc coexistence state. Starting with the α phase after heating, the inset of Fig. 2(a) shows the slightly broadened lattice spot, with weak parasitic scattering from surface imperfections. Closer to the interface, humps of diffuse scattering at $q = 0.003a^*$ are observed, corresponding to a weak spatial correlation with residual short range order [Fig. 2(a)]; six narrow diffuse streaks are observed along the six directions at $\pm 10°$ from the three a^* axes. A real time study is performed upon heating using the FRELON camera and the fine x-ray beam at a fixed position [Fig. 2(b)]. In the α phase, before the occurrence of the diffuse scattering, only the usual lattice spot (exhibited by the curve labeled α) is observed. Then the evolution of the diffuse scattering curves [labeled from (1) to (8)] is monitored during a linear heating ramp of 0.03 K in 6 min. From (1) to (5), the boundary B_{inc} moves up, the lattice peak broadens, and two shoulders appear and develop into two broad humps. On curve (6), the curved B_{inc} interface reaches the x-ray beam and sharp satellites appear at $q = 0.006a^*$. Only six satellites are first observed corresponding to a single rotation domain [(6) to (8)]; the second family of rotation domains (with six other satellites) is observed a little farther from the interface, as shown in Fig. 2(c). The lattice and satellite spots are all broadened by coexistence strains; however, the fine structure of the rotation domains is well resolved, allowing an accurate measurement of the thermal variations of q during heating, as shown by curve (C') of Fig. 1(a). Curve (C'') shows the
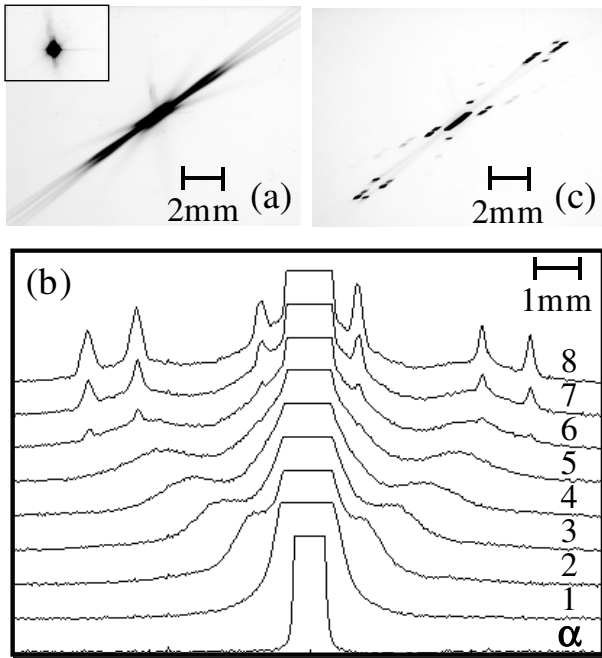
FIG. 2. Spatially resolved investigation of the α-inc coexistence state of the sample Sx using a fine x-ray beam (0.3×0.1 mm^2). (a) A photographic picture of the diffuse streaks around the (012) Laue spot obtained at 0.35 mm above B_{inc}, in the static coexistence state (after heating). Inset: the (012) Laue spot in the α phase, 2 mm above B_{inc}. (b) Real time study of the variations of the diffuse scattering upon heating, using the FRELON camera and a fixed x-ray beam. The curves are obtained as a function of time, by the projection of the diffuse intensity pattern [similar to (a)] on the common bisecting direction. (c) The same conditions as in (a) but obtained in the inc phase 0.4 mm below B_{inc}, exhibiting the 12 satellites of the inc phase.

subsequent variation of q upon cooling, exhibiting a thermal hysteresis reduced to 0.24 K and a final jump of $q = 0.002a^*$ (10 times smaller than the equilibrium value at T_c). In both cases, ϕ saturates around 10°.

The exact correspondence between B_{op} and B_{inc} is determined by simultaneous optical and x-ray measurements. The direct optical observation of sample Sx indicates already a fair correspondence between B_{op} and B_{inc}. In order to check the reproducibility of our previous measurements, we first performed a spatially resolved x-ray study on the second sample Ny (not shown here). Then a simultaneous x-ray and LS study performed on Ny upon cooling gives a detailed picture of the interface region. The temperature decreases slowly during the first 20 min and then remains constant. As a very slow motion of the α-inc interface is going on, the relevant parameter for this study is time, which is used as the abscissa in Fig. 3 for the variations of both q and the LSs intensity. The initial boundary of the SAS region corresponds to the sharp increase of the SAS intensity, clearly within the inc phase but without any specific feature in the x-ray pattern. The position of B_{inc} determined by the final discontinuity of $q = 0.002a^*$ cor-
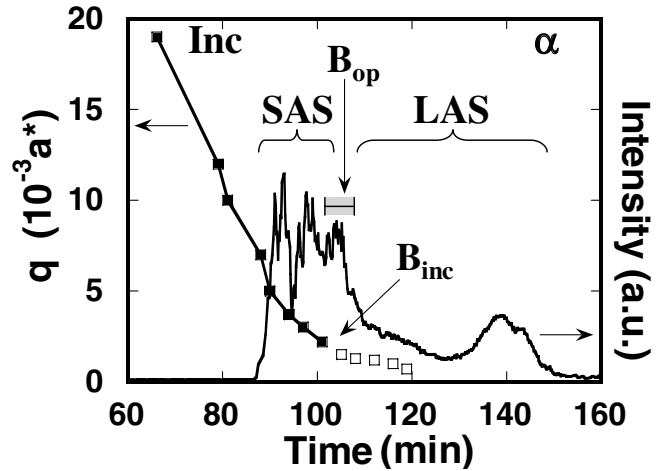

FIG. 3. Time evolutions of the simultaneous x-ray diffraction and light scattering measurements during the nearly isothermal motion of the α-inc phase boundary (after cooling) performed on the sample Ny. The solid squares show the decrease of q in the usual $3q$ inc phase (the line is only a guide to the eye). The open squares correspond to the position of the diffuse short range order hump. The full line exhibits the time variation of the intensity of the light scattered from the laser beam.

responds to the position of the optical boundary B_{op} between the SAS and LAS regions (with an uncertainty of 0.2 mm resulting from the apparent width of B_{op}). The x-ray diffuse humps and streaks are observed in the first part of the LAS region, with a weak maximum of the diffuse scattering around $q = 0.001a^*$. Because of the broadening of the lattice spot, the diffuse x-ray scattering could not be observed farther from the phase boundary, and it disappears before the final sharp decrease of the LAS. Upon heating, as the discontinuity of $q = 0.006a^*$ is larger, the width of the region of the diffuse x-ray scattering is larger and closer to that of the LAS region.

These fine beam studies determine clearly the position and the nature of the LS regions on the two sides of the boundary of the $3q$ inc phase. The previous controversy on their structure (based on TEM observations) and on the origin of LS is now discussed in the light of the present results. Saint-Grégoire *et al.* [11] first proposed that SAS is due to the ferroelastic properties of blocks of two dimensional periodic elongated triangles (2D-ELT), which they observed by TEM. This model was criticized by Aslanyan *et al.* [12] who proposed the existence of another ferroelastic inc phase related to a new commensurate phase with a tripling of the elementary cell, necessary in their model to produce an intense LS. In both models, the new inc phases are considered as equilibrium phases, existing in a small temperature range above T_c. This is not compatible with the present results. As the tripling of the elementary cell, proposed by Aslanyan *et al.* [12], was observed neither in TEM [20] nor in the present x-ray experiments, we do not consider this model anymore. The third model, namely, the coexistence model [6], is based on the systematic observations of LS occurring in the α-inc coexistence state: SAS is

attributed to the nonequilibrium properties of the inc rotation domains in the vicinity of the phase boundary while LAS is attributed to the extensive presence of the transition domains of the α phase (called Dauphiné twins in quartz), also perturbed by the presence of the phase boundary.

In the framework of the coexistence model, we now compare our structural observations to the great variety of triangular structures obtained by TEM [4,13–15]. In the $3q$ inc phase, the various TEM investigations show good reproducibility, even close to the low temperature phase boundary, where high contrast rotation domains of equilateral triangles (EQT) are observed, with wall distances ($d = 45$–60 nm) and rotation angles ($\phi = 10°$) larger than in the pure inc phase at T_c ($d = 20$ nm, $\phi = 7°$) [6]. However, on the α phase side of the EQT boundary, greater differences are observed: a frequent scenario [4,13,14] consists in the apparition of irregular ELT followed by larger Dauphiné twins, showing the wall rotations predicted by Walker [21]. The most organized ELT patterns are obtained by Snoeck and Roucau, exhibiting, however, some variations. Under a large temperature gradient, the whole range of the inc phase between the α and β phases is observed [15]: on the α phase side of the well defined boundary of the EQT structure, linear ELT patterns are observed presenting weak short range order; the limit with the homogeneous α phase is marked by a single layer of large ELT of variable sizes but with parallel walls, rotated by $\pm 10°$ from one of the a^* axes. This picture is in striking agreement with our diffuse x-ray scattering measurements (Fig. 2). However, under a smaller temperature gradient, Snoeck and Roucau observed a 2D-ELT pattern with well defined periodicities, between the α phase and the EQT blocks of the $3q$ inc phase [11,22]. In macroscopic samples, our x-ray results exclude the presence of large blocks of a well ordered 2D-ELT phase, not only above T_c but also in the coexistence state. On the other hand, the presence of small 2D-ELT blocks with short range order is compatible with the diffuse x-ray scattering observed on the α phase side of B_{inc}, contributing then to LAS. Because of the sensitivity to the experimental conditions, a direct and simple extrapolation of the TEM results to macroscopic samples is rather hazardous. With TEM, the sample thickness and the width of the interfacial regions are smaller than 1 μm, while in macroscopic samples they are in the mm range. In the same way, the size of the EQT rotation domains increases from less than 1 μm in TEM to 100 μm and more in x-ray experiments.

Several scenarios are proposed in Ref. [6] for the origin of LS. For LAS, the proposed effects of large rotation domains, with discontinuous variations of q, are in good agreement with the present x-ray and LS results. The LS mechanism of perturbed Dauphiné twins is less evident, but variations of the order parameter, in the interfacial triangular structures observed in TEM [15,22], are suggested in Ref. [6] and by Saint-Grégoire [23]. The difficult question of the origin of these inhomogeneous structures, probably present to decrease the interface energy, would need a complex model coupling anisotropic elasticity and a nonlinear variation of the order parameter.

In conclusion, the combination of spatially resolved optical and x-ray measurements on high quality quartz crystal is necessary to determine unambiguously the microscopic structure of the macroscopic regions producing the transition opalescence of quartz in the α-inc coexistence state. A well defined boundary of the $3q$ inc phase exhibits a final discontinuity of q and defines the limit between SAS and LAS regions. SAS is produced in the $3q$ inc phase by rotation domains, while LAS is produced in the α phase by Dauphiné microtwins, both with perturbed properties, in agreement with the coexistence model.

---

*Corresponding author.
E-mail: gerard.dolino@ujf-grenoble.fr

[1] A. D. Bruce and R. A. Cowley, *Structural Phase Transitions* (Taylor and Francis, London, 1981).

[2] A. Planes and L. Mañosa, Solid State Phys. **55**, 159 (2001).

[3] J. Bornarel and R. Cach, Phys. Rev. B **60**, 3806 (1999).

[4] P. J. Heaney, Rev. Miner. **29**, 1 (1994).

[5] I. A. Yakolev et al., Sov. Phys. Crystallogr. **1**, 91 (1956).

[6] G. Dolino and P. Bastie, J. Phys. Condens. Matter **13**, 11 485 (2001).

[7] S. M. Shapiro and H. Z. Cummins, Phys. Rev. Lett. **21**, 1578 (1968).

[8] G. Dolino and J.-P. Bachheimer, Phys. Status Solidi A **41**, 673 (1977); G. Dolino, Phys. Status Solidi A **60**, 391 (1980).

[9] G. Dolino et al., Solid State Commun. **45**, 295 (1983); K. Gouhara et al., J. Phys. Soc. Jpn. **52**, 3697 (1983).

[10] T. A. Aslanyan and A. P. Levanyuk, JETP Lett. **28**, 70 (1979).

[11] P. Saint-Grégoire et al., JETP Lett. **64**, 410 (1996).

[12] T. A. Aslanyan et al., J. Phys. Condens. Matter **10**, 4577 (1998).

[13] G. van Tendeloo et al., Phys. Status Solidi A **33**, 723 (1976); J. van Landuyt et al., Phys. Rev. B **31**, 2986 (1985).

[14] N. Yamamoto et al., J. Phys. Soc. Jpn. **57**, 1352 (1988).

[15] E. Snoeck and C. Roucau, Phys. Rev. B **45**, 12 720 (1992).

[16] P. Bastie et al., J. Phys. D **36**, A139 (2003).

[17] J.-C. Labiche et al., ESRF Newsletter **25**, 41 (1996).

[18] F. Mogeon et al., Phys. Rev. Lett. **62**, 179 (1989); V. Soula et al., Phys. Rev. B **48**, 6871 (1993).

[19] V. Soula et al., Phys. Rev. B **46**, 626 (1992).

[20] P. Saint-Grégoire et al., Ferroelectrics **252**, 1 (2001).

[21] M. B. Walker, Phys. Rev. B **28**, 6407 (1983).

[22] P. Saint-Grégoire et al., Ferroelectrics **290**, 97 (2003).

[23] P. Saint-Grégoire, Ferroelectrics **240**, 139 (2000).